Differential Sialylation Modulates Voltage-gated Na^+ Channel Gating throughout the Developing Myocardium

Patrick J. Stocker and Eric S. Bennett

Department of Physiology and Biophysics and Program in Neuroscience, University of South Florida College of Medicine, Tampa, FL 33612

Voltage-gated sodium channel function from neonatal and adult rat cardiomyocytes was measured and compared. Channels from neonatal ventricles required an ~10 mV greater depolarization for voltage-dependent gating events than did channels from neonatal atria and adult atria and ventricles. We questioned whether such gating shifts were due to developmental and/or chamber-dependent changes in channel-associated functional sialic acids. Thus, all gating characteristics for channels from neonatal atria and adult atria and ventricles shifted significantly to more depolarized potentials after removal of surface sialic acids. Desialylation of channels from neonatal ventricles did not affect channel gating. After removal of the complete surface N-glycosylation structures, gating of channels from neonatal atria and adult atria and ventricles shifted to depolarized potentials nearly identical to those measured for channels from neonatal ventricles. Gating of channels from neonatal ventricles were unaffected by such deglycosylation. Immunoblot gel shift analyses indicated that voltage-gated sodium channel α subunits from neonatal atria and adult atria and ventricles are more heavily sialylated than α subunits from neonatal ventricles. The data are consistent with approximately 15 more sialic acid residues attached to each α subunit from neonatal atria and adult atria and ventricles. The data indicate that differential sialylation of myocyte voltage-gated sodium channel α subunits is responsible for much of the developmental and chamber-specific remodeling of channel gating observed here. Further, cardiac excitability is likely impacted by these sialic acid–dependent gating effects, such as modulation of the rate of recovery from inactivation. A novel mechanism is described by which cardiac voltage-gated sodium channel gating and subsequently cardiac rhythms are modulated by changes in channel-associated sialic acids.

The Journal of General Physiology

INTRODUCTION

Voltage-gated sodium channels, Na_v, are responsible for the initiation and propagation of action potentials in excitable tissues, opening rapidly and then inactivating after a membrane depolarization (Hille, 2001). The orchestrated activation and inactivation of Na_v is vital to normal skeletal muscle and neuronal function, and in maintaining normal heart rhythm. Slight changes in channel function may cause myotonia, paralysis, epilepsy, long QT syndrome (LQTS), idiopathic ventricular fibrillation (IVF), heart failure, or other cardiac conduction disorders (Bennett et al., 1995; Wang et al., 1995; Keating and Sanguinetti, 1996; Priori et al., 1999; Chen et al., 1998; Green et al., 1998; Bendahhou et al., 1999; Makita et al., 2000; Wehrens et al., 2000; Abriel et al., 2001; Nuyens et al., 2001; Ufret-Vincenty et al., 2001a; Wallace et al., 2001; Splawski et al., 2002; Spampanato et al., 2004).

To date, reports indicate that several α subunit isoforms are expressed variably throughout the heart, including, $Na_{v1.1}$, $Na_{v1.3}$, $Na_{v1.4}$, $Na_{v1.5}$, and $Na_{v1.6}$ (Rogart et al., 1989; Dhar Malhotra et al., 2001; Maier et al., 2002, 2004; Haufe et al., 2005). However, data indicate that $Na_{v1.5}$ is the major current-carrying α subunit expressed in the sarcolemma (Maier et al., 2002; Zimmer and Benndorf, 2002; Haufe et al., 2005). Thus, apparently, $Na_{v1.5}$ is primarily responsible for the initiation and propagation of action potentials resulting in ventricular systole.

Na_v are typically heavily glycosylated with up to 35% of their total mass attributed to carbohydrate (Messner and Catterall, 1985; Roberts and Barchi, 1987; Schmidt and Catterall, 1987; Gordon et al., 1988; Cohen and Levitt, 1993). A large percentage of these sugars are sialic acid (SA) residues (Roberts and Barchi, 1987). Reports have indicated that SA, which is negatively charged at physiological pH, may play a role in channel function. Nearly identical depolarizing shifts in $Na_{v1.4}$ gating were observed using three independent methods to reduce channel sialylation (Bennett et al., 1997).

Another study showed that sialic acid directly altered Na_v gating in an isoform-specific manner (Bennett, 2002). All measured $Na_{v1.4}$ gating parameters were shifted by a depolarizing 11–15 mV when $Na_{v1.4}$ was undersialylated, while sialic acid had no significant effect on $Na_{v1.5}$ gating. These observations were confirmed

Correspondence to Eric Bennett: esbennet@hsc.usf.edu

Abbreviations used in this paper: CHO, Chinese hamster ovary; IVF, idiopathic ventricular fibrillation; LQTS, long QT syndrome; MLP, muscle LIM protein; SA, sialic acid.

through converse chimeric analysis in which the $Na_{v1.4}$ IS5-S6 loop was replaced by the analogous $Na_{v1.5}$ loop (hSkM1P1) and vice versa (hH1P1). Gating phenotypes were switched, with hSkM1P1 gating independently of sialic acid, while hH1P1 gating was generally sialic acid dependent. These experiments provided two novel findings: (1) removal/creation of sialic acid sensitivity to $Na_{v1.4}$/$Na_{v1.5}$, respectively, verifies that for this system, $Na_{v1.4}$ is sialic acid sensitive while $Na_{v1.5}$ is insensitive; and (2) functional sialic acids in this system are localized to the $Na_{v1.4}$ IS5-S6 loop. Thus, sialic acids attached to the $Na_{v1.4}$ IS5-S6 loop are necessary and sufficient to impose a uniform electrostatic effect on channel gating, while $Na_{v1.5}$ sialic acids had no measurable effect on channel gating. While sialic acids in this system apparently worked through an electrostatic mechanism, sialic acids might impose electrostatic and structural effects on channel gating, as previously suggested for $K_{v1.1}$ (Watanabe et al., 2003).

Interestingly, while previous data indicated that SA had no impact on $Na_{v1.5}$ gating as expressed in Chinese hamster ovary (CHO) cells, chemical desialylation of $Na_{v1.5}$ expressed in HEK 293 cells resulted in depolarizing shifts in V_a (Zhang et al., 1999; Bennett, 2002). Because the effects of sialic acid on channel gating vary with the expression system used, studies of Na_v function in cardiomyocytes would most directly address whether sialic acid alters cardiac Na_v gating.

Previous studies have suggested that channel glycosylation may impact heart function. Desialylation via neuraminidase treatment increased L and T-type Ca^{2+} currents in rabbit sino-atrial nodal cells and ventricular myocytes (Fermini and Nathan, 1991; Marengo et al., 1998). Neuraminidase treatment of adult mouse ventricular myocytes altered the voltage dependence and conductance of transient outward K^+ and fast inward Na^+ currents and reduced the number of rat cardiac M_2 muscarinic agonist–receptor complexes (Haddad et al., 1990; Ufret-Vincenty et al., 2001a,b).

Here we examined the differences in Na_v gating between neonatal and adult cardiomyocytes from atria and ventricles under conditions of full and reduced sialylation and N-glycosylation. We find that the majority of differences in Na_v gating between neonatal heart chambers and throughout the developing ventricle can be accounted for by differential glycosylation, with changes in functional sialylation the most dominant effect. A model by which this differential sialylation might alter cardiac excitability most notably through significant modulation of Na_v recovery from inactivation is proposed.

MATERIALS AND METHODS

Cardiac Myocyte Isolation and Culture

Myocytes were isolated from male neonatal (3–5 d) and adult (10–12 wk) Sprague-Dawley rats. The neonatal myocyte isolation protocol was adapted from a method previously described (Isenberg and Klockner, 1982). In detail, neonatal rats were anaesthetized with pentobarbital sodium (200 mg/kg). Atrial or ventricular tissue was dissected out and washed in Ca^{2+}-free Tyrodes solution and then separated into individual myocytes by immersion in 0.1% collagenase (Sigma-Aldrich type I) solution for 0.5 h, centrifuged for 5 min at 160 *g*, and then retreated with fresh collagenase solution for 1 h. Tissue was triturated to disperse myocytes. The myocyte-rich collagenase solution was centrifuged, rinsed with Krebs–HEPES bicarbonate solution, centrifuged again, and then plated with culture media. Adult ventricular and atrial myocytes were isolated using a Langendorf perfusion protocol (7–10 ml/min) adapted from a method previously described (Saint et al., 1992). Adult rats were anaesthetized with pentobarbital sodium (200 mg/kg) and hearts were then dissected out. Whole hearts were first perfused with Ca^{2+}-free Tyrodes for 5 min, then with 300 U/ml collagenase (Sigma-Aldrich type I) and 280 μg/ml protease (Sigma-Aldrich type XIV) in Ca^{2+}-free Tyrodes for 12 min, followed by 5 min of 0.1 mmol/liter Ca^{2+} Tyrodes. Atrial/ventricular tissue was then removed and triturated in 0.1 mmol/liter Ca^{2+} Tyrodes, run through a 200 μm filter, rinsed three times with culture media, and then plated. Cells were used for electrophysiological experiments within 72 h of plating. All chemicals, reagents, enzymes, and animal tissue were stored, used, and disposed of following guidelines outlined in product literature, and established and approved by the USF Institutional Animal Care and Use Committee (IACUC).

Whole-cell Recording of Rat Cardiomyocyte Sodium Currents

Cardiomyocytes were studied using the patch-clamp whole-cell recording technique previously described (Bennett et al., 1997). Experiments were done using an Axon Instruments 200B patch-clamp amplifier with a CV203BU headstage (Axon Instruments) used in combination with a Nikon TE200 inverted microscope. The pulse protocols were generated using a Pentium II computer (Dell Computers) running pulse acquisition software (HEKA). The resulting analogue signals were filtered at 5 kHz using an eight-pole Bessel filter (9200 LPF; Frequency Devices) and then digitized using the ITC-16 AD/DA converter (Instrutech). A micromanipulator (MP-285 Sutter) was used to place the electrode on the cell. Electrode glass (Drummond capillary tubes) was pulled using a Sutter (model P-87) electrode puller to resistances of 1–2 MΩ.

Whole-cell recording extracellular solution was (in mmol/liter) 5 NaCl, 10 tetraethylsulfamide (TES), 5 KCl, 1 $CaCl_2$, 5 CsCl, 10 glucose, 115 choline chloride. The electrode solution was (in mmol/liter) 120 CsF, 10 TES, 2 $MgCl_2$, 2 $CaCl_2$, 5 NaCl, 20 EGTA. Using these salt solutions, similar average current densities were measured for each cell type. No current densities were impacted significantly by neuraminidase treatment, consistent with our previous work that suggested channel conductance is not significantly affected by desialylation (Bennett et al., 1997).

To ensure proper space clamping of the myocyte, several measures were taken. (1) Data were analyzed from cells producing sodium currents of 7 nA or less and reversing near the predicted sodium reversal potential. This required using solutions that contained only 5 mM NaCl. (2) Only myocytes of 76 pF or less were analyzed to ensure space clamp fidelity. (3) The slopes of the G-V Boltzmann relationships were monitored, and only cells in which the slope was >5 mV were analyzed. Any steeper slope indicated a loss of voltage clamp. (4) All analyzed data were collected between 8–12 min after achieving whole-cell configuration.

In addition, all data were series resistance compensated to 95–98%. If proper compensation was not achieved, the data were not analyzed. All experiments were performed at room temperature (~22°C).

TABLE I

Gating Parameters for Na_v from Neonatal and Adult Cardiomyocytes under Conditions of Full and Reduced Sialylation/Glycosylation

Myocyte type	Treatment	*n*	V_a	V_i	τ_h at −50 mV	τ_{rec} at −120 mV
			mV	mV	ms	ms
Neonatal ventricle	Control/Untreated	11	−46.1 ± 1.0	−87.8 ± 1.5	4.0 ± 0.2	7.9 ± 0.3
	Neuraminidase	11	−46.8 ± 1.0[a]	−88.7 ± 1.2[a]	4.9 ± 0.4[a]	7.9 ± 0.6[a]
	PNGase-F	6	−49.5 ± 1.5[a]	−90.6 ± 1.1[a]	3.6 ± 0.3[a]	8.4 ± 0.6[a]
Adult ventricle	Control/Untreated	8	−56.9 ± 1.1[c]	−97.1 ± 2.7[c]	2.8 ± 0.1[c]	13.7 ± 1.9[c]
			U[c]; N[a]	U[c]; N[a]	U[c]; N[a]	U[c]; N[c]
	Neuraminidase	8	−47.3 ± 1.6	−83.8 ± 2.1	4.7 ± 0.7	5.4 ± 0.7
			U[c]; N[a]	U[c]; N[a]	U[c]; N[a]	U[c]; N[a]
	PNGase-F	7	−48.3 ± 2.0	−86.7 ± 2.6	3.7 ± 0.5	7.6 ± 0.7
Neonatal atrium	Control/Untreated	17	−57.0 ± 0.6[c]	−100.0 ± 0.7[c]	2.2 ± 0.1[c]	18.1 ± 1.2[c]
			U[c]; N[a]	U[b]; N[c]	U[c]; N[c]	U[c]; N[c]
	Neuraminidase	13	−49.9 ± 1.1	−95.4 ± 1.8	3.2 ± 0.2	13.2 ± 1.7
			U[c]; N[a]	U[c]; N[a]	U[c]; N[a]	U[c]; N[a]
	PNGase-F	6	−47.2 ± 2.0	−86.3 ± 2.0	4.5 ± 0.6	8.0 ± 0.9
Adult atrium	Control/Untreated	13	−56.7 ± 1.0[c]	−96.7 ± 1.5[c]	2.0 ± 0.1[c]	14.5 ± 1.5[c]
			U[c]; N[a]	U[c]; N[a]	U[c]; N[c]	U[c]; N[a]
	Neuraminidase	11	−49.9 ± 1.0	−91.3 ± 0.9	3.3 ± 0.2	9.7 ± 0.8
			U[c]; N[a]	U[c]; N[a]	U[c]; N[a]	U[c]; N[a]
	PNGase-F	7	−50.0 ± 1.0	−88.8 ± 1.9	3.0 ± 0.3	9.9 ± 1.2

The mean gating parameter values ± SEM are listed. V_a, voltage of half-activation; V_i, Voltage of half-inactivation; τ_h, fast inactivation time constant; τ_{rec}, time constant for recovery from fast inactivation. Significance was determined using a two-tailed Student's *t* test comparing sample groups as follows: (1) untreated samples were compared to untreated neonatal ventricular myocytes, (2) treated samples were compared to their untreated cell type (U), and neonatal ventricular myocytes (N).

[a]Not significant.

[b]Significant ($P < 0.02$).

[c]Highly significant ($P < 0.01$).

Desialylation/Deglycosylation of Cardiomyocytes

To remove sialic acids, cells were plated onto 35-mm dishes and exposed to 1.125–1.5 U neuraminidase (Sigma-Aldrich type X)/ml Dulbecco's modified Eagle's medium for 3 h at 37°C. To remove N-glycosylation, cells were exposed to 19–20 U PNGase-F (Sigma-Aldrich)/ml Dulbecco's modified Eagle's medium for 12 h at 37°C. Each glycosidase is relatively specific. The neuraminidase will break α2-3, α2-6, and, to a lesser extent, α2-8 linkages of sialic acids attached to carbohydrate structures. PNGase-F is very specific for breaking the linkage between N-acetylglucosamine and the asparagine residue to which it is attached.

Pulse Protocols

Conductance–Voltage (G-V) Relationship. Pulse protocols were performed as previously described using a –120 mV holding potential (Bennett, 2002). The cells were stepped for 10 ms from the holding potential to various depolarized potentials, ranging from –100 to +40 mV in 10-mV increments. Consecutive pulses were stepped every 1.5 s and the data were leak subtracted using the P/4 method, stepping negatively from the holding potential. At each test potential, steady-state whole-cell conductance was determined by measuring the peak current at that potential and dividing by the driving force (i.e., difference between the membrane potential and the observed reversal potential). Peak conductance as a function of membrane potential was plotted. The maximum sodium conductance for a single cell was determined following single Boltzmann fits to the data (Eq. 1, solving for maximum conductance). The average V_a ± SEM values listed in Table I are determined from these data fits. As illustrated in Figs. 2 and 6, there are no obvious differences in the K_a ± glycosidase treatment, and therefore K_a values are not listed in Table I. Statistical comparisons of K_a ± glycosidase treatment showed no significant differences ($P < 0.02$), and the measured K_a ± SEM for untreated, neuraminidase-treated, and PNGase-F treated, respectively, were (in mV): (1) neonatal atria: 8.6 ± 0.2, 8.9 ± 0.4, and 8.1 ± 0.6; (2) adult atria: 7.7 ± 0.3, 8.2 ± 0.3, and 8.2 ± 0.6; (3) neonatal ventricle: 9.2 ± 0.5, 9.0 ± 0.3, and 8.0 ± 0.4; and (4) adult ventricle: 7.0 ± 0.4, 6.0 ± 0.3, and 7.4 ± 0.3.

From the Boltzmann fits, the normalized data were then averaged with those from other cells, and the resultant average conductance–voltage curve was determined using the following Boltzmann relation fit to the data:

$$\text{Fraction of maximal conductance} = \left[1 + \left(\exp - \left(V - V_a/K_a\right)\right)\right]^{-1}, \quad (1)$$

where V is the membrane potential, V_a is the voltage of half activation, and K_a is the slope factor.

Steady-state Inactivation Curves (h_{inf}). Cells were first prepulsed for 500 ms from the holding potential to the plotted potentials ranging from –130 to –20 mV in 10-mV increments, then to a +40 mV test pulse for 5 ms. Currents from each cell were normalized to the maximum current measured by single Boltzmann fits to the data from a single cell (Eq. 2, solving for maximum current), from which the mean V_i ± SEM values listed in Table I were determined. As illustrated in Figs. 3 and 6, there are no obvious differences in the K_i ± glycosidase treatment, and therefore K_i values are not listed in Table I. Statistical comparisons of K_i ± glycosidase treatment showed no significant differences ($P < 0.02$), and the measured K_i ± SEM for untreated, neuraminidase-treated, and PNGase-F treated, respectively, were (in mV): (1) neonatal atria: –7.2 ± 0.2, –7.8 ± 0.2, and –7.9 ± 0.6; (2) adult atria: –7.2 ± 0.2, –7.8 ± 0.2, and –8.0 ± 0.4; (3) neonatal ventricle: –7.9 ± 0.2, –7.8 ± 0.4, and –8.6 ± 0.5; and (4) adult ventricle: –7.8 ± 0.3, –8.1 ± 0.3, and –7.1 ± 0.4.

From the Boltzmann fits, the normalized data for many cells were then averaged and the following Eq. 2 was fit to these data to produce the least squares fit curves shown in Fig. 1 B, Fig. 3, and Fig. 6 B:

$$\text{Fraction of maximum current} = \left[1 + \left(\exp\left((V - V_i)/K_i\right)\right)\right]^{-1}, \quad (2)$$

where V is the membrane potential, V_i is the voltage of half inactivation, and K_i is the slope factor.

Measurement of Inactivation Time Constants (τ_h). Inactivation time constants were determined by fitting to single exponential functions the attenuating portions of the current traces used to measure the G-V relationships.

Recovery from Inactivation. Cells were held at −120 mV, pulsed to +40 mV for 10 ms, and then stepped to the recovery potential for 1–20 ms in 1-ms increments. After the recovery pulse, the potential was again stepped to +40 mV for 10 ms. The peak currents measured during the two +40 mV depolarizations were compared to determine the fractional current (recovery) measured during the second pulse. The fractional current was plotted as a function of the recovery time (in ms) between the two test pulses to +40 mV (Fig. 1 D, inset, labeled as I/I_o). Single exponential functions were fit to the data to determine the time constants for recovery from fast inactivation, τ_{rec}.

Immunoblot

Cellular homogenates were made by first harvesting the appropriate tissues (neonatal and adult cardiac atrial/ventricular muscle). The tissue was placed in ice cold sodium pyrophosphate buffer containing protease inhibitors (20 mmol/liter tetrasodium pyrophosphate, 20 mmol/liter Na_2PO_4, 1 mmol/liter $MgCl_2$, 0.5 mmol/liter EDTA, 300 mmol/liter sucrose, 0.8 mmol/liter benzamidine, 1 mmol/liter iodacetamide, 1.1 μmol/liter leupeptin, 0.7 μM pepstatin, 76.8 nM aprotinin), and homogenized using a Polytron homogenizer (Brinkmann Instruments model PT10/35), set at 10, pulsed several times to ensure complete homogenization, and then stored at −80°C. Samples were mixed with sample buffer (10% glycerol, 5% 2-mercaptoethanol, 3% SDS, 12.5% upper Tris buffer [upper Tris buffer is 500 mM Tris, 0.4% SDS, pH 6.8]), denatured for 2 min in boiled water, and then loaded into the lanes of a minigel cast from 4.5% acrylamide. The gel was run for its full length at 75–100 V and then electrophoretically transferred to nitrocellulose paper using a semi-dry transfer cell (Bio-Rad Laboratories) for 22 min at 8–14 V. Treated homogenates were incubated with 1.35 U neuraminidase/10 μg protein for 3 h at 37°C to remove sialic acids, and with 19–20 U PNGase-F (Sigma-Aldrich)/10 μg protein for 12 h at 37°C to remove N-glycosylation structures. Cardiac sodium channel α subunits were detected using a 1:200 dilution of a site-directed polyclonal pan-specific antibody previously described (αAb) (Bennett, 1999), and then incubated with donkey anti-rabbit horseradish peroxidase–conjugated secondary antibody (Amersham Biosciences) for 2 h, and visualized using a Pierce Chemical Co. enhanced chemiluminescence kit.

Data Analysis

All electrophysiological data were analyzed using Pulse/PulseFit (HEKA) and Sigmaplot 2001 (SSPS Inc.) software. Sigmagel (SSPS Inc.) software was used to quantify the immunoblot data.

RESULTS

Na_v from Neonatal Ventricles Gate at More Depolarized Potentials

Whole-cell Na^+ currents similar to those shown in Fig. 1 A were recorded from single neonatal and adult cardiomyocytes from atria and ventricles to determine developmental and chamber-specific differences in Na_v gating. Biophysical analyses revealed that gating of Na_v from neonatal atria and adult atria and ventricles occurred after smaller depolarizations than did gating of Na_v from neonatal ventricles (Fig. 1, A–D). Steady-state channel activation (G-V; Fig. 1 A) and inactivation (h_{inf}; Fig. 1 B) curves for Na_v from neonatal atria and adult atria and ventricles were 9–10 mV more hyperpolarized than those measured for channels from neonatal ventricles (Fig. 1, A and B). The fast inactivation time constants (τ_h) measured for Na_v from neonatal atria and adult atria and ventricles were smaller (faster) than τ_h for Na_v from neonatal ventricles (Fig. 1 C).The time to recovery from fast inactivation (τ_{rec}) is slower for Na_v from neonatal atria and adult atria and ventricles than for Na_v from neonatal ventricles (Fig. 1 D). Collectively, these data reveal a consistent chamber-specific difference in neonatal Na_v gating, and a hyperpolarization in Na_v gating as the ventricle develops. The mean values ± SEM for all voltage-dependent gating parameters measured in this report are listed in Table I.

Steady-state Gating of Na_v from Neonatal Atria and Adult Atria and Ventricles Are Sensitive to Desialylation while Na_v Gating in the Neonatal Ventricle Is Insensitive

Na_v gating was studied under conditions of full and reduced sialylation to determine whether the observed chamber-specific and developmental shifts in gating could be attributed to differences in functional channel sialylation. Fig. 2 shows G-V curves for Na_v from each myocyte type ± SA (surface SA removed by treating with neuraminidase). Note that the G-V curves for Na_v from neonatal atria and adult atria and ventricles treated with neuraminidase were shifted in the depolarized direction by a significant 7–10 mV, while neuraminidase treatment had no effect on the G-V relationship for Na_v from neonatal ventricles.

Desialylation similarly altered steady-state inactivation, with neuraminidase causing a significant 5–13 mV shift in h_{inf} curves for channels from neonatal atria and adult atria and ventricles, with no effect on steady-state inactivation of channels from neonatal ventricles (Fig. 3).

Sialic Acids Increase Inactivation Rate; Only τ_h for Na_v from Neonatal Ventricles Is Insensitive to Sialic Acids

Fig. 4 shows that desialylation slowed the rate of fast inactivation for Na_v from neonatal atria and adult atria and ventricles (Fig. 4, A, B, and D) with little or no effect on the τ_h measured for Na_v from neonatal ventricles (Fig. 4 C). Note, similar to that observed for steady-state gating, desialylation shifted the τ_h curves toward τ_h measured for channels from neonatal ventricles (which are neuraminidase insensitive).

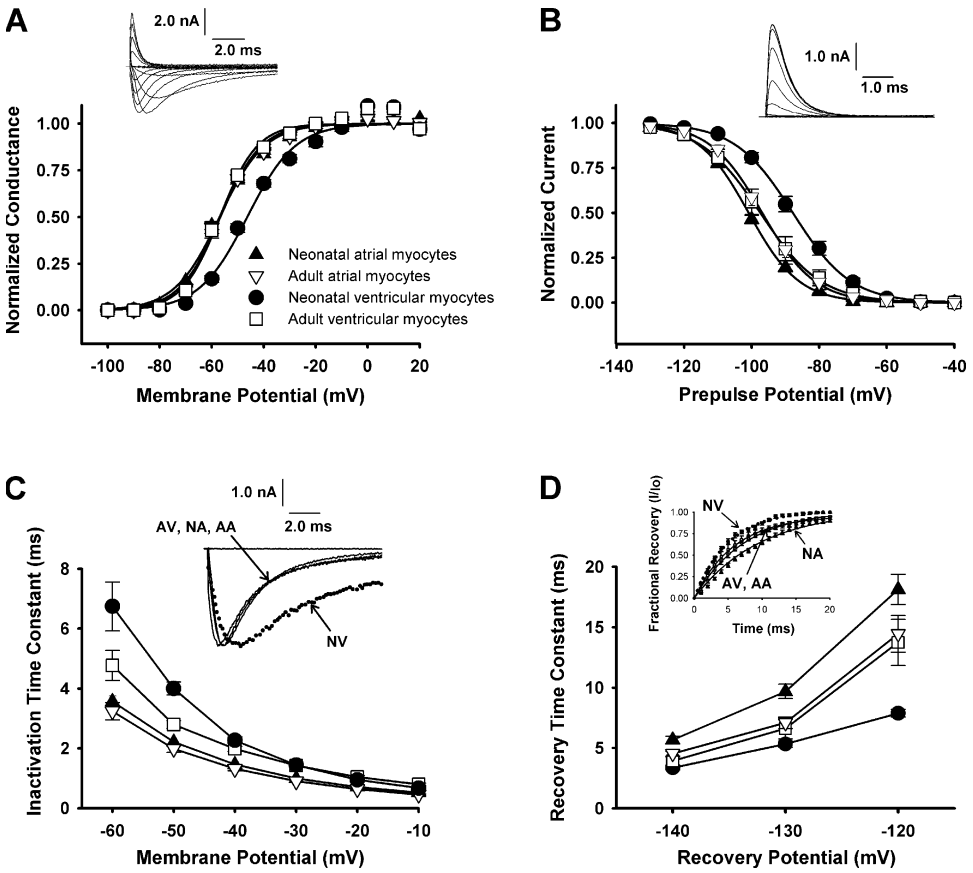

Figure 1. Na_v from neonatal ventricles gate at more depolarized potentials. Filled circles, neonatal ventricular myocytes (NV); open squares, adult ventricular myocytes (AV); filled triangles, neonatal atrial myocytes (NA); open inverted triangles, adult atrial myocytes (AA). The number of samples for each is listed in Table I. (A) Steady-state activation (G-V relationships). Data are the average normalized peak conductance ± SEM at a membrane potential. Curves are single Boltzmann distribution fits to the data. Inset, whole cell Na^+ current from an isolated adult ventricular myocyte. Currents were measured during test pulses of −100 to +40mVin10-mVincrementsfrom the −120 mV holding potential. (B) Steady-state inactivation (h_{inf}). Data are the average peak current ± SEM measured during a 5-ms pulse to +40 mV following a 500-ms prepulse to the plotted potentials. Curves are single Boltzmann distribution fits to the data. Inset, whole cell Na^+ currents measured during a series of +40 mV test pulses, each following a prepulse to a larger depolarization ranging from −130 to −20mV in 10-mV increments. (C) Time constant of fast inactivation (τ_h). Data are the average τ_h ± SEM measured at the plotted potentials. Curves are nontheoretical point-to-point. Inset, current traces during a −50 mV test pulse. Solid traces, NA, AA, and AV. Dotted trace, NV. (D) Voltage dependence of the recovery time constants. Data are the measured time constants for recovery from inactivation (τ_{rec}) ± SEM as a function of recovery potential. Lines are nontheoretical point-to-point. Inset, plotted recovery data and fits for all four conditions at a −130 mV recovery potential. Curves are single exponential function fits to the data. Solid curves, NA, AA, and AV. Dotted curve, NV.

Sialic Acids Slow the Rate of Recovery from Fast Inactivation for Na_v from All Myocyte Types Except Neonatal Ventricles

Fully sialylated Na_v from neonatal atria and adult atria and ventricles consistently recovered from inactivation more slowly than did Na_v from neonatal ventricles (Fig. 1 A). After desialylation, Na_v recovery time decreased for all but Na_v from neonatal ventricles (Fig. 5), toward those values measured for Na_v from neonatal ventricles (Table I).

Removal of N-glycosylation Can Account for Gating Differences among Na_v Expressed throughout the Developing Myocardium

While the SA-induced shifts in gating observed can account for the majority of differences in voltage-dependent Na_v gating among myocyte types studied here, they do not fully account for these differences. One possible reason for this is that neuraminidase treatment, while consistent in removing some functional SA from Na_v, failed to remove all functional sugars. To test this, we attempted to remove the complete N-glycosylation structures from surface channels by treatment with PNGase-F. As shown in Fig. 6, PNGase-F treatment caused all gating characteristics for channels from neonatal atria and adult atria and ventricles to be nearly identical to those observed for Na_v from neonatal ventricles (which were SA and PNGase-F insensitive). In fact, after PNGase-F treatment, no significant differences among myocyte types were observed for any Na_v gating parameter (Table I).

The Na_v α Subunits from Neonatal Atria and Adult Atria and Ventricles Are More Heavily Sialylated than the α Subunit from Neonatal Ventricles

Figs. 2–5 indicate that gating of Na_v from neonatal atria and adult atria and ventricles are more sensitive to desialylation than are Na_v from neonatal ventricles. One possibility is that the Na_v from neonatal ventricles is the least sialylated channel type, with changes in channel

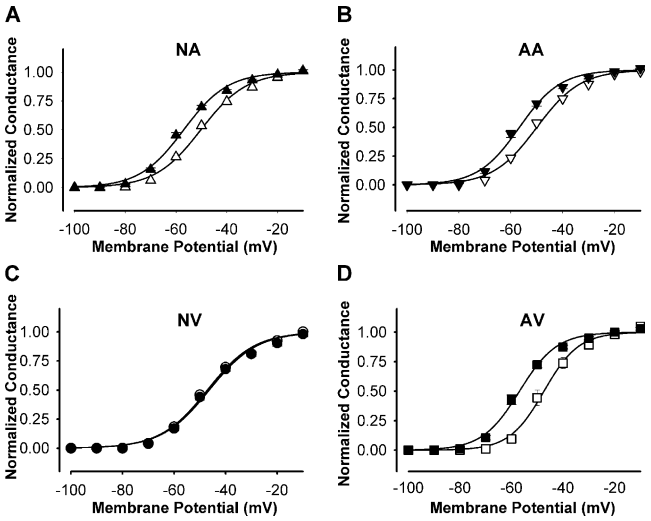

Figure 2. Desialylation of Na_v from neonatal atria and adult atria and ventricles causes a depolarizing shift in steady-state activation; only channels from neonatal ventricles are unaffected. G-V relationships for Na_v ± neuraminidase. Data are the average normalized peak conductance ± SEM at a membrane potential. Curves are single Boltzmann distribution fits to the data. Filled symbols, control/untreated. Open symbols, neuraminidase-treated. Triangles, NA (A). Inverted Triangles, AA (B). Circles, NV (C). Squares, AV (D). The number of samples for each is listed in Table I.

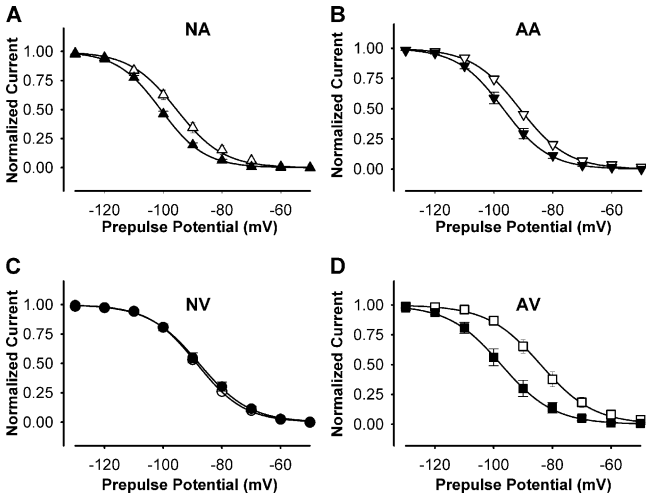

Figure 3. Desialylation shifts steady-state inactivation curves for Na_v from neonatal atria and adult atria and ventricles but has no effect on inactivation of channels from neonatal ventricles. Steady-state inactivation (h_{inf}) for Na_v ± neuraminidase. Data are the average normalized peak current ± SEM measured during a 5-ms test pulse to +40 mV after a 500-ms prepulse to the plotted potentials. Curves are single Boltzmann distribution fits to the data. Filled symbols, control/untreated. Open symbols, neuraminidase-treated. Triangles, NA (A). Inverted Triangles, AA (B). Circles, NV (C). Squares, AV (D). The number of samples for each is listed in Table I.

sialylation levels occurring throughout the developing ventricle and between the newborn's chambers. To test this possibility, multiple immunoblots were run to measure the apparent molecular weight (M_r) of Na_v α subunits expressed in the four myocyte types (Fig. 7). From these blots, it was apparent that the Na_v α subunits from neonatal atria and adult atria and ventricles were similar in M_r, and were consistently more massive than the α subunit from neonatal ventricles (Fig. 7 A). The average measured M_r for α subunits from neonatal atria and adult atria and ventricles was 251.8 ± 0.6 kD (n = 41), versus 246.5 ± 0.8 kD (n = 19) for the α subunit from neonatal ventricles. Thus, α subunits from neonatal atria and adult atria and ventricles were an average ~5 kD larger than the α subunit from neonatal ventricles. Because the α subunit M_r observed for all four homogenates was significantly greater than the predicted M_r for unprocessed $Na_{v1.5}$ (~227 kD), the data indicate that all four α subunits are glycosylated, with the α subunit from neonatal ventricles being the least processed.

To determine more directly whether changes in channel glycosylation were responsible for the observed differences in M_r, myocyte homogenates were treated with PNGase-F to remove N-linked glycosylation at the site of attachment to the channel. The M_r for all four PNGase-F–treated α subunits were reduced to an average 231.1 ± 0.9 kD (n = 20), with no significant difference in M_r measured among the PNGase-F–treated α subunits (Fig. 7 B). These data indicate that the α subunit from neonatal ventricles is ~5 kD less N-glycosylated than the other α subunits.

To question whether the differences in glycosylation levels observed were due to differences in α subunit sialylation, myocyte homogenates were treated

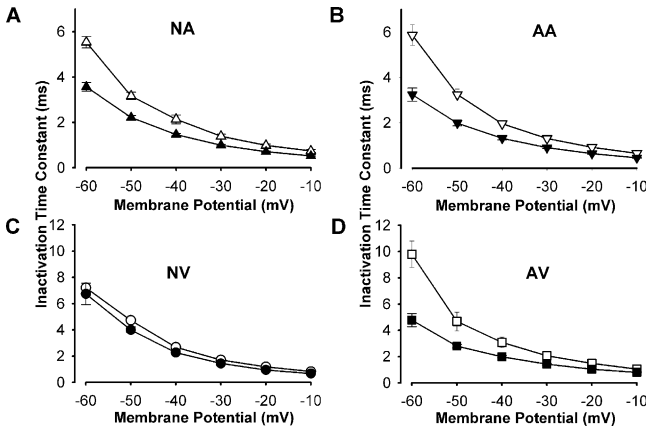

Figure 4. Sialic acid increases the rate of fast inactivation for Na_v from neonatal atria and adult atria and ventricles but has little effect on τ_h for channels from neonatal ventricles. Time constants of fast inactivation (τ_h) ± neuraminidase. Data are the average τ_h ± SEM. Curves are nontheoretical, point-to-point. Filled symbols, control/untreated. Open symbols, neuraminidase-treated. Triangles, NA (A). Inverted Triangles, AA (B). Circles, NV (C). Squares, AV (D). The number of samples for each is listed in Table I.

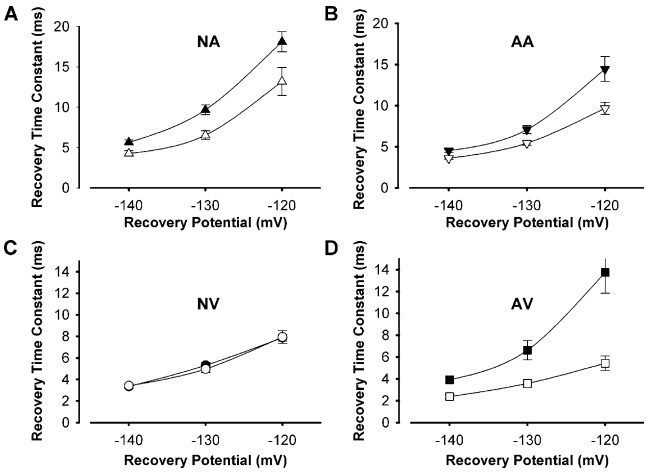

Figure 5. Recovery from fast inactivation for Na_v from neonatal atria and adult atria and ventricles is faster after desialylation; recovery rates of channels from neonatal ventricles are unaffected by sialic acids. Voltage dependence of the time constants for recovery from inactivation ± neuraminidase. Data are the measured τ_{rec} ± SEM as a function of recovery potential. Lines are nontheoretical point-to-point. Filled symbols, control/untreated. Open symbols, neuraminidase treated. Triangles, NA (A). Inverted triangles, AA (B). Circles, NV (C). Squares, AV (D). The number of samples for each is listed in Table I.

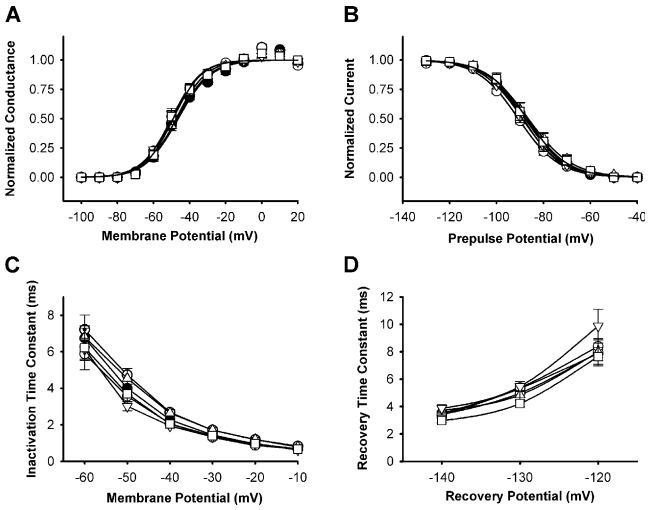

Figure 6. Gating of deglycosylated Na_v from neonatal atria and adult atria and ventricles is nearly identical to gating of channels from neonatal ventricles. Steady-state activation (A) and inactivation (B) relationships and fast inactivation (C) and recovery (D) kinetics are shown for all channel types after treatment with PNGase-F (open symbols: triangles, NA; inverted triangles, AA; circles, NV; squares, AV), and for Na_v from neonatal ventricles under control/untreated (solid circles) and neuraminidase-treated (dotted, open circles) conditions. Data are the mean ± SEM. Number of samples for each is listed in Table I.

with neuraminidase to remove sialic acids specifically (Fig. 7 C). The α subunit M_r for all homogenates were reduced to similar levels following neuraminidase treatment, suggesting that all α subunits are sialylated, with the α subunits from neonatal atria and adult atria and ventricles being more sialylated than the α subunit from neonatal ventricles. Fig. 7 D illustrates the average α subunit M_r measured under control, PNGase-F, and neuraminidase-treated conditions (listed in Table II). The graph shows that the M_r for untreated α subunits from neonatal atria and adult atria and ventricles were nearly identical, while M_r for untreated α subunits from neonatal ventricles was significantly smaller. The M_r for each channel type was reduced to similar levels after treatment with each glycosidase. This indicates that a difference in channel sialylation is primarily responsible for the differences in α subunit M_r observed. On average, SA-dependent M_r (change in M_r with neuraminidase treatment) was ~5.3 kD for the α subunit from neonatal ventricles and a much larger 9.1 kD (72% increase) for the α subunits from each of the other myocyte types. In fact, direct comparison indicated a highly significant, 3.8 ± 0.4 kD larger SA-dependent shift in M_r ($n = 23$) for α subunits from neonatal atria and adult atria and ventricles than for α subunits from neonatal ventricles. This is consistent with ~15 more sialic acid residues attached to the α subunits from neonatal atria and adult atria and ventricles than to α subunits from neonatal ventricles.

DISCUSSION

Remodeling of Na_v Gating throughout the Developing Myocardium Is Dependent on Differential Na_v Sialylation

Here, we observed that voltage-dependent steady-state and kinetic gating events for Na_v from neonatal and adult atria and ventricles were shifted in the hyperpolarized direction by ~10 mV compared with the gating characteristics of Na_v from neonatal ventricles. We sought to explore what might be responsible for this Na_v remodeling. We hypothesized that developmental and/or chamber-dependent changes in channel-associated functional sialic acids may account for some of these gating shifts. Neuraminidase treatment was used to remove sialic acids attached to surface Na_v. None of the voltage-dependent gating characteristics for Na_v from neonatal ventricles were affected by neuraminidase treatment, while all gating characteristics for Na_v from neonatal atria and adult atria and ventricles were shifted to more depolarized potentials, toward those measured for Na_v from neonatal ventricles.

Removal of N-linked sugars via PNGase-F treatment (Fig. 6) caused all gating characteristics for Na_v from neonatal atria and adult atria and ventricles to behave nearly identically to those measured for channels from neonatal ventricles (control and glycosidase treated). There are likely inherent differences in Na_v gating among myocyte types in addition to those described

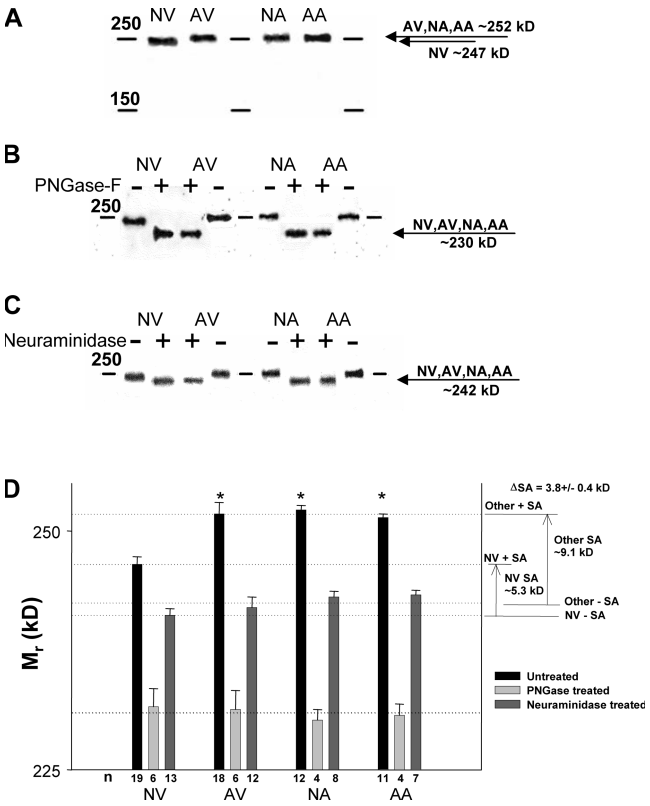

Figure 7. Gel shift analyses indicate that α subunit sialylation increases throughout the developing myocardium. Bands detected using αAb at a 1:200 concentration. Lane labels: NV, neonatal ventricle; AV, adult ventricle; NA, neonatal atria; AA, adult atria. (A) Immunoblot of Na_v α subunits from neonatal and adult atria and ventricles. Lanes 1, 4, and 7, molecular weight markers; lane 2, NV; lane 3, AV; lane 5, NA; lane 6, AA. Protein loaded per lane: 5 μg. (B) Immunoblot of Na_v α subunits from neonatal and adult atria and ventricles ± PNGase-F treatment. Lanes 1, 6, and 11, molecular weight markers; lane 2, NV; lane 3, NV + PNGase-F; lane 4, AV + PNGase-F; lane 5, AV; lane 7, NA; lane 8, NA + PNGase-F; lane 9, AA + PNGase-F; lane 10, AA. Protein loaded per lane: control/untreated, 5 μg; PNGase-F-treated, 10 μg. (C) Immunoblot of Na_v α subunits from neonatal and adult atria and ventricles ± neuraminidase treatment. Lanes 1, 6, and 11, molecular weight markers; lane 2, NV; lane 3, NV + neuraminidase; lane 4, AV + neuraminidase; lane 5, AV; lane 7, NA; lane 8, NA + neuraminidase; lane 9, AA + neuraminidase; lane 10, AA. Protein loaded per lane: control/untreated, 5 μg; neuraminidase treated, 10 μg. (D) Bar graph of average measured Na_v α subunit M_r ± PNGase-F ± neuraminidase. Each bar represents the mean M_r ± SEM measured for a series of immunoblots. Dark bars, untreated; light bars, PNGase-F treated; gray bars, neuraminidase treated. The number of samples measured is listed at the base of each bar. Significance was determined for the untreated data using a two-tailed Student's *t* test comparing the M_r for the α subunit from neonatal ventricles to the M_r for the α subunits from neonatal atria and adult atria and ventricles. *, significant ($P < 0.01$).

here (e.g., effects of differential sympathetic input on Na_v gating, see Zhang et al., 1992). However, our data, at a minimum, suggest that the majority of differences in Na_v gating between neonatal heart chambers, and throughout the developing ventricle can be accounted for by differential glycosylation, with changes in functional sialylation the most dominant effect. That is, functional SA, defined here as the measurable SA-dependent effects on channel gating, account for the majority of differences in voltage-dependent gating of Na_v among the myocyte types studied. Removal of the full N-glycosylation structures could account for all measured shifts in gating among Na_v. It is possible that two distinct N-glycosylation–dependent mechanisms are responsible for the sugar-induced hyperpolarizing shifts in Na_v gating. However, another likely possibility is that while neuraminidase treatment consistently removed functional sialic acids, it may not have removed all functional sialic acids for each cell studied, while PNGase-F treatment was much more effective at removing functional sialic acids.

Previously, we showed that $Na_{v1.5}$ gating can be affected by trans sialic acids attached to the β_1 subunit (Johnson et al., 2004). It is known that β_1 expression increases with the developing ventricle. Our immunoblot data indicate a significant increase in β_1 expression for adult ventricles compared with the adult atria and neonatal atria and ventricles (the adult atria and neonatal atria and ventricles expressed similar levels; unpublished data). We explored the possibility that β_1 sialic acids might be fully responsible for the shifts in gating for channels from adult ventricles. β_1 overexpressed in neonatal ventricular myocytes had no effect on Na_v steady-state activation or inactivation ($n = 4$; data not shown), suggesting that simply adding β_1 to the α subunit is not sufficient to produce the SA-dependent hyperpolarization observed throughout the developing ventricle.

Immunoblot analyses indicated that Na_v α subunits from neonatal atria and adult atria and ventricles were more heavily sialylated than α subunits from neonatal ventricles (Fig. 7). Gel shift studies predicted that ~15 fewer SA are attached to the α subunits from neonatal ventricles. While the immunoblot data indicate that the α subunits from neonatal ventricles are sialylated (albeit significantly less sialylated), the sialic acids were not measurably functional. This is consistent with our previous study comparing effects of sialic acids on $Na_{v1.4}$ and $Na_{v1.5}$ gating in CHO cells (Bennett, 2002). We found that while $Na_{v1.5}$ is apparently glycosylated as expressed in CHO cells, no functional effects of sugars on gating were observed. Evidently here, with a 72% increase in the number of sialic acids attached to α subunits from neonatal atria and adult atria and ventricles, SA-dependent function becomes measurable. Given this, the biochemical data are consistent with the biophysical measurements, suggesting that much of the differences in gating between Na_v from neonatal ventricles and Na_v from neonatal atria and adult atria and ventricles are the result of differential levels of functional sialylation.

TABLE II

Gel Shift Analyses for Na_v from Neonatal and Adult Cardiomyocytes under Conditions of Full and Reduced Glycosylation/Sialylation

Myocyte type	Untreated (n)	PNGase-F (n)	Neuraminidase (n)
Neonatal ventricle	246.5 ± 0.8 (19)	231.6 ± 1.9 (6)[a]	241.2 ± 0.7 (13)[a]
Adult ventricle	251.8 ± 1.2 (18)[a]	231.3 ± 2.0 (6)[a]	242.0 ± 1.1 (12)[a]
Neonatal atria	252.2 ± 0.5 (12)[a]	230.2 ± 1.1 (4)[a]	243.1 ± 0.6 (8)[a]
Adult atria	251.4 ± 0.4 (11)[a]	230.7 ± 1.2 (4)[a]	243.3 ± 0.5 (7)[a]

Data list the mean apparent molecular weight (M_r; in kD) ± SEM measured for neonatal and adult cardiomyocyte Na_v α subunits. The number of samples, *n*, for each is listed in parentheses. For the untreated data, significance was determined using a two-tailed Student's *t* test comparing the α subunit M_r from neonatal atria and adult atria and ventricles to the α subunit M_r from neonatal ventricles. The same test for significance was used comparing treated homogenates to untreated controls.
[a]Highly significant ($P < 0.01$).

Apparently, the numbers/locations of functional sialic acids added to Na_v are regulated as a function of development and cardiac region.

In summary, Na_v from neonatal ventricles are apparently less functionally sialylated than Na_v from neonatal atria and adult atria and ventricles, and this reduced sialylation is responsible for much of the chamber-specific and development-dependent differences in Na_v gating observed here.

Differential Sialylation Modulates Na_v Gating through Two Different Mechanisms

Previous data from our laboratory indicated that various Na_v α subunits are differently glycosylated/sialylated as expressed in the same cell line. This difference in α subunit sialylation directly and differently alters channel gating (Bennett, 2002). Thus, channel gating is partially dependent on the "glycosylation signature" of the α subunit expressed. The number and/or location of sialic acids vary among α subunits, producing a potential spectrum of functional sialic acids among α subunits that may directly and differently modulate channel gating acutely.

The data shown here are consistent with a second "cell-specific" mechanism by which differential channel sialylation modulates Na_v gating. We show that Na_v gating throughout the developing ventricle shifts in the hyperpolarized direction because the adult Na_v α subunit is apparently more heavily sialylated than the α subunit from neonatal ventricles. One possible explanation for this increased sialylation would be a chronic increase in sialyltransferase activity in the developing ventricles. Also, greater sialyltransferase activity in the newborn atria versus ventricle might explain the increase in atrial α subunit functional sialylation. Consistently, our recent GeneChip microarray analysis of the developing myocardium indicated significant developmental and chamber-specific differences in sialyltransferase expression (unpublished data).

Thus, as the model in Fig. 8 illustrates, we predict two mechanisms by which differential sialylation might alter Na_v gating: (1) subunit specific (Bennett, 2002), and (2) cell specific (as suggested here). Each mechanism might produce a set of sugar-dependent gating motifs. The combining of the two mechanisms would increase the number of putative gating motifs dramatically, effectively modulating Na_v function by creating a spectrum of Na_v that gate at different voltages.

It may be inferred from the model shown in Fig. 8 that the rate of modulation of Na_v gating through subunit- and cell-specific differential sialylation would be limited by the rate of protein synthesis. That is, expression of a specific channel and the specific sialyltransferases active in the Golgi as that channel is trafficked through the Golgi together will determine the level/location of functional channel sialylation. However, there is evidence that for other cell types, such modulation may take place on a more dynamic time scale. For example, internalized surface proteins might reenter directly into the Golgi glycosylation pathway (Snider and Rogers, 1986; Brandli and Simons, 1989; Jin and Snider, 1993). If this occurs in cardiomyocytes, then a differently sialylated channel might be produced through a process that would be faster than one requiring de novo protein synthesis. Also, more rapid differential sialylation might be achieved through ecto-sialyltransferase activity. Ecto-sialyltransferases were shown to be responsible for changes in transmembrane protein surface sialylation in certain cell types (Taatjes et al., 1988; Gross et al., 1996; Kaufmann et al., 1999; Schwartz-Albiez et al., 2004). If such a mechanism is involved in cardiomyocytes, then these ecto-sialyltransferases might produce rapid adjustments to surface channel sialylation. Thus, if these two mechanisms are involved in cardiac physiology, the rate of modulation of Na_v gating imposed through differential channel sialylation might occur across a spectrum of rates, ranging from relatively rapid differential ecto-sialyltransferase activity to the much slower rate of protein synthesis.

Developmental Effects of Differential Sialylation May Be Tissue Specific

Differential sialylation appears to be a mechanism by which cardiac Na_v activity can be modulated throughout development or between cardiac chambers. We observed essentially uniform hyperpolarizing shifts in each Na_v gating parameter with development of the ventricle that was linked to increasing channel sialylation. A recent study of $Na_{v1.9}$ in rat dorsal root ganglia also reported developmental regulation of channel sialylation. The apparently more heavily sialylated neonatal $Na_{v1.9}$ inactivated at more hyperpolarized potentials than did the adult $Na_{v1.9}$. Channel activation voltage was unaffected (Tyrrell et al., 2001). Interestingly, these opposing changes in dorsal root ganglion $Na_{v1.9}$ and

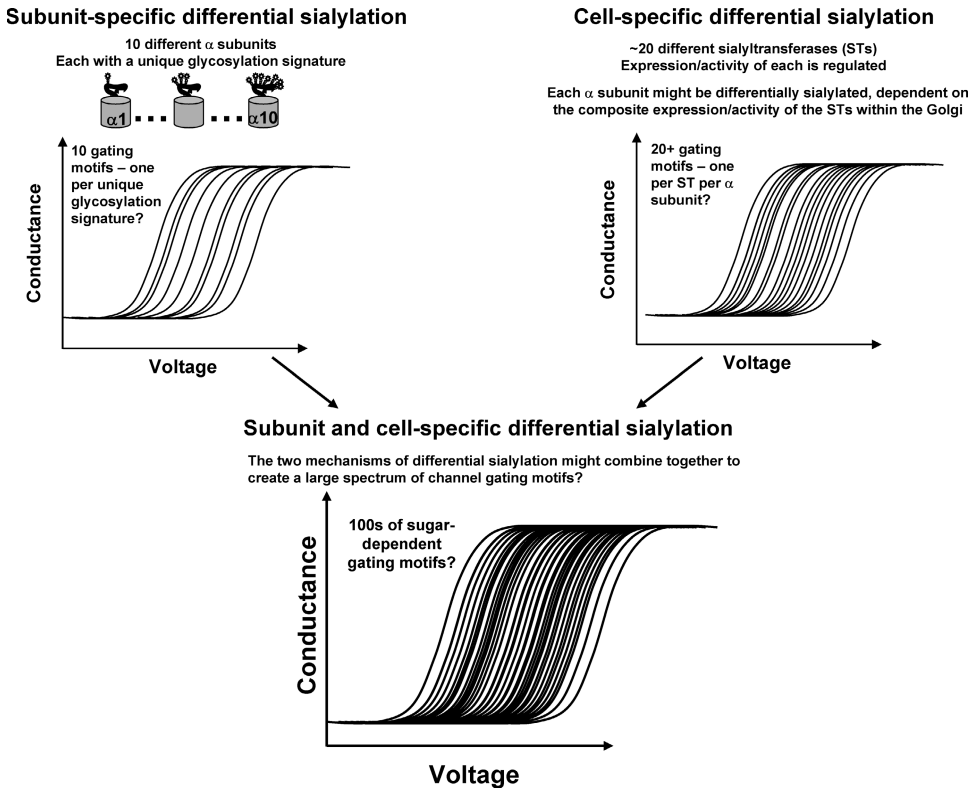

Figure 8. Is Na_v gating modulated through two complementary mechanisms of differential sialylation? Model depicts subunit- and cell-specific differential sialylation. Each mechanism potentially can produce a modest spectrum of channel gating motifs (shown for illustrative purposes only, as different G-V relationships). Top left panel, subunit-specific differential sialylation. Each α subunit will have an inherent "glycosylation signature" that predetermines the level/location of glycosylation that can be attached to that α subunit. Top right panel, cell-specific differential sialylation. The relative activity of one to several of the 20 STs will determine the amount and location of sialic acids added to one α subunit. When combined together (bottom), perhaps hundreds of gating motifs could be realized. For example, by assuming that each of the 10 Na_v α subunits might be sialylated differently by the activity of each of the 20 known STs, 200 different gating motifs might be possible. This model is likely oversimplified, as it does not account for the even greater number of gating motifs that might be realized through activity of multiple STs in various combinations, or for the varied expression/activity of other glycosylation-related genes. Thus, with the regulated expression of specific α subunits combined with the regulated expression and activity of specific STs, Na_v gating might be modulated across a large and finely tuned spectrum of voltages.

cardiac Na_v sialylation throughout the development of two different cell types suggest that channel gating is modulated chronically through tissue-specific differential sialylation. In addition, these uniform gating shifts for differentially sialylated cardiac Na_v versus the non-uniform shifts (only V_i was affected) for $Na_{v1.9}$ suggest that the modulation of Na_v gating through cell-specific differential sialylation may be isoform specific.

Differential Sialylation Modulates the Rate of Recovery from Fast Inactivation and the Window Current, thereby Likely Impacting Cardiac Excitability

Here we show that Na_v gating is altered by the addition of functional sialic acids to channels throughout development of the ventricle. In addition, Na_v from neonatal atria have a greater level of functional sialic acids than do Na_v from neonatal ventricles. What might be the physiological role for such developmental and chamber-specific remodeling? The changes in Na_v gating observed here, such as shifts in the window current voltage range and changes in the rate of recovery from inactivation, previously were implicated in causing increased susceptibility to arrhythmias and/or reentrant excitation that lead to several cardiac disorders including LQTS (Abriel et al., 2001; Nuyens et al., 2001), IVF (Chen et al., 1998), and heart failure (Ufret-Vincenty et al., 2001a).

The distribution of channels between the open and inactivated states at a membrane potential represented graphically by overlapping G-V and h_{inf} curves is referred to as the "window current" (Attwell et al., 1979). The intersecting area under the curves represents the voltage range at which a small percentage of channels are persistently active. For the Na_v from neonatal atria and adult atria and ventricles, the window current voltage range is ~10 mV more hyperpolarized than is the window current voltage range for the Na_v from neonatal ventricles, caused primarily by SA-dependent hyperpolarizing shifts in the G-V and h_{inf} curves (Fig. 1, A and B). Once desialylated/deglycosylated, the window current voltage ranges for Na_v from neonatal atria and adult atria and ventricles were shifted in the depolarized direction, to similar voltage ranges as that observed for channels from neonatal ventricles (Figs. 2, 3, and 6). Previous reports suggest that point mutations of SCN1A and SCN5A resulting in similar shifts in the window current voltage range as observed here with desialylation/deglycosylation may be responsible for such maladies as epilepsy and arrhythmias (LQTS) (Abriel et al., 2001; Spampanato et al., 2004).

While our data indicate an SA-dependent shift in window current voltage range that apparently impacts persistent Na^+ channel activity, we also observe a remarkable SA-dependent slowing of the rate of recovery from fast inactivation for all but the channels from neonatal ventricles. That is, as shown in Figs. 5 and 6, Na_v from neonatal atria and adult atria and ventricles recover from fast inactivation more slowly than do channels from neonatal ventricles. This SA-dependent slower recovery rate will act to increase the effective time between successive depolarizing/repolarizing waves because of the redistribution of Na_v toward a larger population of inactivated channels. Previous reports have suggested that faster recovery rates increase the probability of reentrant excitation or early afterdepolarizations, possibly resulting in LQT-3 (Nuyens et al., 2001) or in IVF (Chen et al., 1998). In fact, Chen et al. (1998) suggested that SCN5A mutations that were responsible for a 25–30% faster recovery rate at a −80 mV recovery potential might cause IVF. The authors showed that this difference in recovery rate between wild type and the mutant SCN5A attenuated with more hyperpolarized recovery potentials, becoming insignificant at recovery potentials more negative than −110 mV. Here we report a much larger SA-dependent effect on recovery rate. At a −120 mV recovery potential, the rate of recovery from inactivation for the less sialylated Na_v from neonatal ventricles is 40–60% faster than for the more heavily sialylated channels from neonatal atria and adult atria and ventricles (Table I). Thus, our data indicate that the differential sialylation of Na_v throughout the developing myocardium may have a greater impact on the rate of recovery from fast inactivation than do SCN5A mutation(s) that lead to IVF.

A recent study suggested a role for sialic acids in cardiomyocyte excitability (Ufret-Vincenty et al., 2001a). Cardiac excitability and Na_v gating were studied using a mouse model for heart failure, a knockout of the muscle LIM protein (MLP). Neuraminidase treatment of control (wild type) ventricular myocytes produced Na^+ currents with steady-state gating characteristics similar to those of untreated, but apparently less sialylated, $MLP^{-/-}$ myocytes. This suggested that the extended action potential repolarization of the $MLP^{-/-}$ myocyte was caused, at least in part, by Na_v with reduced sialylation. There was a reduction and rightward shift in the window current of the Na_v from $MLP^{-/-}$ myocytes and also for Na_v from the neuraminidase-treated control myocytes. In addition, the rate of fast inactivation was slowed for Na_v from desialylated and $MLP^{-/-}$ myocytes. The action potential duration in $MLP^{-/-}$ myocytes was prolonged, and these myocytes were more susceptible to early afterdepolarizations. The authors concluded that the apparently lesser sialylated Na_v from $MLP^{-/-}$ myocytes might be responsible for these changes in myocyte excitability. Interestingly, both the rightward shift in window current voltage range and the slower inactivation rates described for Na_v from $MLP^{-/-}$ myocytes are consistent with that observed here for all desialylated channels and for treated and untreated channels from neonatal ventricles.

Thus, the probable net role for Na_v differential sialylation is to help regulate and modulate cardiac rhythms achieved through SA-dependent shifts in Na_v window current and/or SA-dependent changes in the rate of recovery from inactivation.

Summary

Here we show a developmental and chamber-specific role for cell-specific differential sialylation in cardiomyocyte ion channel function. Functional analyses of cardiomyocyte Na_v showed that Na_v from neonatal atria and adult atria and ventricles gate at more hyperpolarized potentials than do channels from neonatal ventricles. Much of these region-specific and developmental shifts in gating were shown to be sialic acid dependent, with complete removal of N-glycosylation accounting fully for these shifts. This developmental and chamber-specific differential sialylation modulates the rate of Na_v recovery from fast inactivation to a greater extent than does an SCN5A mutation implicated as causal for IVF, further indicating the potential importance of differential Na_v sialylation to cardiac excitability. A complete description of the role of differential sialylation in cardiac excitability throughout the developing myocardium must wait until further investigation determines the effects of differential sialylation on the other ion channels and transporters involved in the varied action potentials observed throughout the developing myocardium.

The authors would like to thank Jean M. Harper for her technical expertise.

This work was supported in part by a grant from the National Institute for Arthritis and Musculoskeletal and Skin Diseases (E.S. Bennett).

Olaf S. Andersen served as editor.

Submitted: 5 October 2005
Accepted: 30 January 2006

REFERENCES

Abriel, H., C. Cabo, X.H. Wehrens, I. Rivolta, H.K. Motoike, M. Memmi, C. Napolitano, S.G. Priori, and R.S. Kass. 2001. Novel arrhythmogenic mechanism revealed by a long-QT syndrome mutation in the cardiac Na^+ channel. *Circ. Res.* 88:740–745.

Attwell, D., I. Cohen, D. Eisner, M. Ohba, and C. Ojeda. 1979. Steady-state Ttx-sensitive (window) sodium current in cardiac Purkinje-fibers. *Pflugers Arch.* 379:137–142.

Bendahhou, S., T.R. Cummins, R. Tawil, S.G. Waxman, and L.J. Ptacek. 1999. Activation and inactivation of the voltage-gated sodium channel: role of segment S5 revealed by a novel hyperkalaemic periodic paralysis mutation. *J. Neurosci.* 19:4762–4771.

Bennett, E., M.S. Urcan, S.S. Tinkle, A.G. Koszowski, and S.R. Levinson. 1997. Contribution of sialic acid to the voltage dependence of sodium channel gating. A possible electrostatic mechanism. *J. Gen. Physiol.* 109:327–343.

Bennett, E.S. 1999. Effects of channel cytoplasmic regions on the activation mechanisms of cardiac versus skeletal muscle Na^+ channels. *Biophys. J.* 77:2999–3009.

Bennett, E.S. 2002. Isoform-specific effects of sialic acid on voltage-dependent Na^+ channel gating: functional sialic acids are localized to the S5-S6 loop of domain I. *J. Physiol.* 538:675–690.

Bennett, P.B., K. Yazawa, N. Makita, and A.L. George. 1995. Molecular mechanism for an inherited cardiac-arrhythmia. *Nature.* 376:683–685.

Brandli, A.W., and K. Simons. 1989. A restricted set of apical proteins recycle through the trans-Golgi network in MDCK cells. *EMBO J.* 8:3207–3213.

Chen, Q., G.E. Kirsch, D. Zhang, R. Brugada, J. Brugada, P. Brugada, D. Potenza, A. Moya, M. Borggrefe, G. Breithardt, et al. 1998. Genetic basis and molecular mechanism for idiopathic ventricular fibrillation. *Nature.* 392:293–296.

Cohen, S.A., and L.K. Levitt. 1993. Partial characterization of the Rh1 sodium-channel protein from rat-heart using subtype-specific antibodies. *Circ. Res.* 73:735–742.

Fermini, B., and R.D. Nathan. 1991. Removal of sialic-acid alters both T-type and L-type calcium currents in cardiac myocytes. *Am. J. Physiol.* 260:H735–H743.

Gordon, D., D. Merrick, D.A. Wollner, and W.A. Catterall. 1988. Biochemical-properties of sodium-channels in a wide-range of excitable tissues studied with site-directed antibodies. *Biochemistry.* 27:7032–7038.

Green, D.S., A.L. George Jr., and S.C. Cannon. 1998. Human sodium channel gating defects caused by missense mutations in S6 segments associated with myotonia: S804F and V1293I. *J. Physiol.* 510(Pt 3):685–694.

Gross, H.J., A. Merling, G. Moldenhauer, and R. Schwartz-Albiez. 1996. Ecto-sialyltransferase of human B lymphocytes reconstitutes differentiation markers in the presence of exogenous CMP-N-acetyl neuraminic acid. *Blood.* 87:5113–5126.

Haddad, E., Y. Landry, and J.P. Gies. 1990. Sialic-acid residues as catalysts for M2-muscarinic agonist-receptor interactions. *Mol. Pharmacol.* 37:682–688.

Haufe, V., J.A. Camacho, R. Dumaine, B. Gunther, C. Bollensdorff, G.S. von Banchet, K. Benndorf, and T. Zimmer. 2005. Expression pattern of neuronal and skeletal muscle voltage-gated Na^+ channels in the developing mouse heart. *J. Physiol.* 564:683–696.

Hille, B. 2001. Ionic Channels of Excitable Membranes. Third edition. Sinauer Associates, Inc. 1–22.

Isenberg, G., and U. Klockner. 1982. Calcium tolerant ventricular myocytes prepared by pre-incubation in a Kb medium. *Pflugers Arch.* 395:6–18.

Jin, M., and M.D. Snider. 1993. Role of microtubules in transferrin receptor transport from the cell surface to endosomes and the Golgi complex. *J. Biol. Chem.* 268:18390–18397.

Johnson, D., M.L. Montpetit, P.J. Stocker, and E.S. Bennett. 2004. The sialic acid component of the β1 subunit modulates voltage-gated sodium channel function. *J. Biol. Chem.* 279:44303–44310.

Kaufmann, M., C. Blaser, S. Takashima, R. Schwartz-Albiez, S. Tsuji, and H. Pircher. 1999. Identification of an α2,6-sialyltransferase induced early after lymphocyte activation. *Int. Immunol.* 11:731–738.

Keating, M.T., and M.C. Sanguinetti. 1996. Pathophysiology of ion channel mutations. *Curr. Opin. Genet. Dev.* 6:326–333.

Maier, S.K., R.E. Westenbroek, K.A. McCormick, R. Curtis, T. Scheuer, and W.A. Catterall. 2004. Distinct subcellular localization of different sodium channel α and β subunits in single ventricular myocytes from mouse heart. *Circulation.* 109:1421–1427.

Maier, S.K., R.E. Westenbroek, K.A. Schenkman, E.O. Feigl, T. Scheuer, and W.A. Catterall. 2002. An unexpected role for brain-type sodium channels in coupling of cell surface depolarization to contraction in the heart. *Proc. Natl. Acad. Sci. USA.* 99:4073–4078.

Makita, N., N. Shirai, D.W. Wang, K. Sasaki, A.L. George Jr., M. Kanno, and A. Kitabatake. 2000. Cardiac Na^+ channel dysfunction in Brugada syndrome is aggravated by β1-subunit. *Circulation.* 101:54–60.

Dhar Malhotra, J., C. Chen, I. Rivolta, H. Abriel, R. Malhotra, L.N. Mattei, F.C. Brosius, R.S. Kass, and L.L. Isom. 2001. Characterization of sodium channel α- and β-subunits in rat and mouse cardiac myocytes. *Circulation.* 103:1303–1310.

Marengo, F.D., S.Y. Wang, B. Wang, and G.A. Langer. 1998. Dependence of cardiac cell Ca^{2+} permeability on sialic acid-containing sarcolemmal gangliosides. *J. Mol. Cell. Cardiol.* 30:127–137.

Messner, D.J., and W.A. Catterall. 1985. The sodium-channel from rat brain: separation and characterization of subunits. *J. Biol. Chem.* 260:10597–10604.

Nuyens, D., M. Stengl, S. Dugarmaa, T. Rossenbacker, V. Compernolle, Y. Rudy, J.F. Smits, W. Flameng, C.E. Clancy, L. Moons, et al. 2001. Abrupt rate accelerations or premature beats cause life-threatening arrhythmias in mice with long-QT3 syndrome. *Nat. Med.* 7:1021–1027.

Priori, S.G., J. Barhanin, R.N.W. Hauer, W. Haverkamp, H.J. Jongsma, A.G. Kleber, W.J. McKenna, D.M. Roden, Y. Rudy, K. Schwartz, et al. 1999. Genetic and molecular basis of cardiac arrhythmias: impact on clinical management. *Eur. Heart J.* 20:174–195.

Roberts, R.H., and R.L. Barchi. 1987. The voltage-sensitive sodium channel from rabbit skeletal muscle. Chemical characterization of subunits. *J. Biol. Chem.* 262:2298–2303.

Rogart, R.B., L.L. Cribbs, L.K. Muglia, D.D. Kephart, and M.W. Kaiser. 1989. Molecular cloning of a putative tetrodotoxin-resistant rat heart Na^+ channel isoform. *Proc. Natl. Acad. Sci. USA.* 86:8170–8174.

Saint, D.A., Y.K. Ju, and P.W. Gage. 1992. A persistent sodium current in rat ventricular myocytes. *J. Physiol.* 453:219–231.

Schmidt, J.W., and W.A. Catterall. 1987. Palmitylation, sulfation, and glycosylation of the α-subunit of the sodium channel: role of posttranslational modifications in channel assembly. *J. Biol. Chem.* 262:13713–13723.

Schwartz-Albiez, R., A. Merling, S. Martin, R. Haas, and H.J. Gross. 2004. Cell surface sialylation and ecto-sialyltransferase activity of human CD34 progenitors from peripheral blood and bone marrow. *Glycoconj. J.* 21:451–459.

Snider, M.D., and O.C. Rogers. 1986. Membrane traffic in animal cells: cellular glycoproteins return to the site of Golgi mannosidase I. *J. Cell Biol.* 103:265–275.

Spampanato, J., J.A. Kearney, G. de Haan, D.P. McEwen, A. Escayg, I. Aradi, B.T. MacDonald, S.I. Levin, I. Soltesz, P. Benna, et al. 2004. A novel epilepsy mutation in the sodium channel SCN1A identifies a cytoplasmic domain for β subunit interaction. *J. Neurosci.* 24:10022–10034.

Splawski, I., K.W. Timothy, M. Tateyama, C.E. Clancy, A. Malhotra, A.H. Beggs, F.P. Cappuccio, G.A. Sagnella, R.S. Kass, and M.T. Keating. 2002. Variant of SCN5A sodium channel implicated in risk of cardiac arrhythmia. *Science.* 297:1333–1336.

Taatjes, D.J., J. Roth, J. Weinstein, and J.C. Paulson. 1988. Post-Golgi apparatus localization and regional expression of rat intestinal sialyltransferase detected by immunoelectron microscopy with polypeptide epitope-purified antibody. *J. Biol. Chem.* 263:6302–6309.

Tyrrell, L., M. Renganathan, S.D. Dib-Hajj, and S.G. Waxman. 2001. Glycosylation alters steady-state inactivation of sodium channel Na(v)1.9/NaN in dorsal root ganglion neurons and is developmentally regulated. *J. Neurosci.* 21:9629–9637.

Ufret-Vincenty, C.A., D.J. Baro, W.J. Lederer, H.A. Rockman, L.E. Quinones, and L.F. Santana. 2001a. Role of sodium channel

deglycosylation in the genesis of cardiac arrhythmias in heart failure. *J. Biol. Chem.* 276:28197–28203.

Ufret-Vincenty, C.A., D.J. Baro, and L.F. Santana. 2001b. Differential contribution of sialic acid to the function of repolarizing K^+ currents in ventricular myocytes. *Am. J. Physiol. Cell Physiol.* 281:C464–C474.

Wallace, R.H., I.E. Scheffer, S. Barnett, M. Richards, L. Dibbens, R.R. Desai, T. Lerman-Sagie, D. Lev, A. Mazarib, N. Brand, et al. 2001. Neuronal sodium-channel α1-subunit mutations in generalized epilepsy with febrile seizures plus. *Am. J. Hum. Genet.* 68:859–865.

Wang, Q., J.X. Shen, I. Splawski, D. Atkinson, Z.Z. Li, J.L. Robinson, A.J. Moss, J.A. Towbin, and M.T. Keating. 1995. Scn5A mutations associated with an inherited cardiac arrhythmia, long QT syndrome. *Cell.* 80:805–811.

Watanabe, I., H.G. Wang, J.J. Sutachan, J. Zhu, E. Recio-Pinto, and W.B. Thornhill. 2003. Glycosylation affects rat Kv1.1 potassium channel gating by a combined surface potential and cooperative subunit interaction mechanism. *J. Physiol.* 550:51–66.

Wehrens, X.H., H. Abriel, C. Cabo, J. Benhorin, and R.S. Kass. 2000. Arrhythmogenic mechanism of an LQT-3 mutation of the human heart Na^+ channel α-subunit: a computational analysis. *Circulation.* 102:584–590.

Zhang, J.F., R.B. Robinson, and S.A. Siegelbaum. 1992. Sympathetic neurons mediate developmental-change in cardiac sodium-channel gating through long-term neurotransmitter action. *Neuron.* 9:97–103.

Zhang, Y., H.A. Hartmann, and J. Satin. 1999. Glycosylation influences voltage-dependent gating of cardiac and skeletal muscle sodium channels. *J. Membr. Biol.* 171:195–207.

Zimmer, T., and K. Benndorf. 2002. The human heart and rat brain IIA Na^+ channels interact with different molecular regions of the β1 subunit. *J. Gen. Physiol.* 120:887–895.